

**A new method for depositing platinum  
exclusively on the internal surface of zeolite L**

Lalchan Persaud, Allen J. Bard, Alan Campion, Marye Anne  
Fox, Thomas E. Mallouk, Stephen E. Webber, and J. M. White

*Inorg. Chem.*, **1987**, 26 (22), 3825-3827 • DOI: 10.1021/ic00269a042

Downloaded from <http://pubs.acs.org> on February 3, 2009

**More About This Article**

---

The permalink <http://dx.doi.org/10.1021/ic00269a042> provides access to:

- Links to articles and content related to this article
- Copyright permission to reproduce figures and/or text from this article



the Cu(II) center, particularly changes in coordination number accompanying loss of ligated water. The bis(diimine) values are closer to the highest apparent self-exchange rate constant ( $k_{22} = 1.3 \times 10^5 \text{ M}^{-1} \text{ s}^{-1}$ ) estimated<sup>22</sup> for the blue copper protein plastocyanin, in which a coordination number change is precluded by the rigid Cu center, held inaccessible to solvent by the enveloping protein. Cu(II)-H<sub>2</sub>O bond breaking does not appear to make a significant contribution to the activation process of the Cu(tmbp)<sub>2</sub><sup>2+</sup> and Cu(dmbp)<sub>2</sub><sup>2+</sup> reactions. The similarity in the  $k_{22}$  values estimated from Cu(tmbp)<sub>2</sub><sup>2+</sup>-Ru(III) and Cu(tmbp)<sub>2</sub><sup>2+</sup>-Ru(II) cross-reaction data also accords with this. The second-order rate constant ( $k_2 = 4 \times 10^5 \text{ M}^{-1} \text{ s}^{-1}$ ) measured for the oxidation of Cu(tmbp)<sub>2</sub><sup>2+</sup> by *cis*-[Ru(NH<sub>3</sub>)<sub>4</sub>(isn)<sub>2</sub>]<sup>3+</sup> yields a value of  $1 \times 10^4 \text{ M}^{-1} \text{ s}^{-1}$  for Cu(tmbp)<sub>2</sub><sup>2+/2+</sup> self-exchange. For the corresponding bipyridyl and phenanthroline couples Cu(bpy)<sub>2</sub><sup>2+/2+</sup> and Cu(phen)<sub>2</sub><sup>2+/2+</sup>, where considerable differences exist in the degree of solvation of the Cu(II) and Cu(I) states, Cu(I)-Cu(I) self-exchange rate constants estimated from Cu(I) oxidation reactions<sup>8</sup> differ considerably from the values obtained from corresponding Cu(II) reductions.<sup>3</sup> A more recent estimate of the Cu(phen)<sub>2</sub><sup>2+/2+</sup> and Cu(bpy)<sub>2</sub><sup>2+/2+</sup> self-exchange rate constants by Anson and Lee,<sup>23</sup> without the simplifying assumption that the Cu(I) oxidant and the Cu(II) reductant make the same contribution to the reorganization energy of the exchange process, has produced  $k_{22} = 1.55 \times 10^4$  and  $4.41 \times 10^3 \text{ M}^{-1} \text{ s}^{-1}$  for the Cu(phen)<sub>2</sub><sup>2+/2+</sup> and Cu(bpy)<sub>2</sub><sup>2+/2+</sup> couples, the latter value being in good agreement with an alternative value they have obtained electrochemically. Somewhat surprising is the similarity between these values and the rate constants estimated for self-exchange in the methyl-substituted counterparts Cu(dmp)<sub>2</sub><sup>2+/2+</sup> and Cu(tmbp)<sub>2</sub><sup>2+/2+</sup>, which show a less than 3-fold rate advantage. It is of interest that the considerable thermodynamic destabilization of the Cu(II) state in sterically constrained methyl-substituted bis(diimine) complexes ( $E^\circ = 0.603$  and  $0.600 \text{ V}$  for Cu(dmp)<sub>2</sub><sup>2+/2+</sup> and Cu(tmbp)<sub>2</sub><sup>2+/2+</sup>;  $E^\circ = 0.174$  and  $0.120 \text{ V}$  for Cu(phen)<sub>2</sub><sup>2+/2+</sup> and Cu(bpy)<sub>2</sub><sup>2+/2+</sup>) is not reflected to a greater degree in the kinetic reorganization barrier to electron transfer between the Cu(I) and Cu(II) states.

**Acknowledgment** is made to the donors of the Petroleum Research Fund, administered by the American Chemical Society, for support of this research.

**Registry No.** Cu(tmbp)<sub>2</sub><sup>2+</sup>, 47718-61-6; Cu(dmbp)<sub>2</sub><sup>2+</sup>, 90316-91-9; [Ru(NH<sub>3</sub>)<sub>2</sub>py](ClO<sub>4</sub>)<sub>2</sub>, 19482-31-6; [Ru(NH<sub>3</sub>)<sub>2</sub>isn](ClO<sub>4</sub>)<sub>2</sub>, 31279-70-6; [Ru(NH<sub>3</sub>)<sub>2</sub>bpy](ClO<sub>4</sub>)<sub>2</sub>, 69793-91-5; *cis*-[Ru(NH<sub>3</sub>)<sub>4</sub>(isn)<sub>2</sub>](ClO<sub>4</sub>)<sub>3</sub>, 31279-74-0.

**Supplementary Material Available:** Tables II-IV, listing kinetic data (3 pages). Ordering information is given on any current masthead page.

Contribution from the Department of Chemistry,  
The University of Texas at Austin, Austin, Texas 78712

### A New Method for Depositing Platinum Exclusively on the Internal Surface of Zeolite L

Lalchan Persaud, Allen J. Bard, Alan Campion,  
Marye Anne Fox, Thomas E. Mallouk,\* Stephen E. Webber,  
and J. M. White

Received November 19, 1986

Natural and synthetic aluminosilicates are of practical importance as molecular sieves and catalysts. Synthetic zeolites modified with nonframework metals are among those materials that have been intensively studied with regard to cation-exchange properties, metal ion localization, and catalysis.<sup>1-3</sup> Transition metal ion exchanged zeolites have been found to be particularly

efficient for various catalytic reactions. For example, oxidation of propylene by cupric ion exchanged zeolite Y,<sup>4</sup> cyclodimerization of butadiene,<sup>5</sup> and the catalytic oxidation of ethylene by Pd<sup>2+</sup>/Cu<sup>2+</sup> metal ions on zeolite Y<sup>6</sup> have been described. Platinized zeolite L has been used in nonacidic catalytic re-forming and dehydrocyclization reactions.<sup>7</sup> Much of this chemistry has focused on creating encapsulated transition-metal catalysts. The principal role of the zeolite framework is to provide a compartmentalized environment, the metal being immobilized within the microporous structure. Molecules that poison the catalyst, if they are sufficiently large, may be size-excluded from the zeolite pore structure.<sup>8</sup> With smaller pore zeolites such as ZSM-5 and ZSM-11, reactant or product selectivity in a metal-catalyzed reaction is achieved by forcing the reactant molecule to pass through the intracrystalline volume in order to contact the metal. Good selectivity is usually obtained by poisoning the metal sites on the external surface with bulky ligands that are too large to access the internal metal sites.<sup>9-11</sup> Intrazeolite reactions are of course highly desirable in shape-selective catalysis since such selectivity may exceed that possible with liquid-phase catalysts.<sup>12</sup>

Some of the charge-balancing counterions of the anionic zeolite framework are readily exchangeable, and the usual route is to introduce metals by equilibration of cationic metal complexes or metal ions with a suspension of the zeolite. Thus Pt and Pd are easily loaded into the large-pore zeolites Y and L by exchanging Na<sup>+</sup> or NH<sub>4</sub><sup>+</sup> ions with Pt(NH<sub>3</sub>)<sub>4</sub><sup>2+</sup> or Pd(NH<sub>3</sub>)<sub>4</sub><sup>2+</sup>.<sup>8,13</sup> Different loadings of noble metal are readily obtained by this ion-exchange method. Transmission electron microscopy and gas adsorption measurements have shown<sup>8,13</sup> that the bulk of the metal deposited is highly dispersed and lies within the zeolite pore structure. We have now prepared, using a neutral platinum complex, zeolite L powders that contain platinum metal exclusively on their inner surfaces. We describe two sensitive chemical tests that can differentiate between zeolites platinized both inside and outside and those platinized only on the inside. To our knowledge, this is the first time that chemical tests have established the absence of metal clusters or particles on the outer surfaces of a metalated zeolite. These platinized zeolite L powders are part of an integrated system for light-driven vectorial electron transport and hydrogen evolution that is described elsewhere.<sup>14</sup>

### Experimental Section

**Materials.** Zeolite L (ideal formula K<sub>6</sub>Na<sub>3</sub>Al<sub>9</sub>Si<sub>27</sub>O<sub>72</sub>·21H<sub>2</sub>O) and zeolite Y (Na<sub>56</sub>Al<sub>56</sub>Si<sub>136</sub>O<sub>384</sub>·250H<sub>2</sub>O) powders were obtained from Union Carbide, Linde Division. Scanning electron microscopy showed that the average particle size was in both cases about 1 μm. Tetraammineplatinum(II) chloride and platinum acetylacetonate (Pt(acac)<sub>2</sub>) were obtained from Strem Chemicals. Methylviologen iodide was prepared

- (1) Sherry, H. S. *Adv. Chem. Ser.* **1971**, No. 101, 350.
- (2) Smith, J. V. *Adv. Chem. Ser.* **1971**, No. 101, 171.
- (3) Naccache, C.; Taarit, Y. B. *Pure Appl. Chem.* **1980**, 52, 2175.
- (4) Mochida, I.; Mayota, S.; Kato, A. *J. Catal.* **1970**, 19, 405.
- (5) Maxwell, I. E.; Downing, R. S.; Von Lauger, S. A. *J. Catal.* **1980**, 61, 485.
- (6) Arai, H.; Yamashiro, T.; Kobo, T.; Tominaga, H. *Bull. Jpn. Pet. Inst.* **1976**, 18, 39.
- (7) (a) Bernard, J. *Proc. Int. Conf. Zeolites* **1980**, 5, 686. (b) Tauster, S. J.; Steger, J. J.; Fung, S. C.; Poeppelmeier, K. R.; Funk, W. G.; Montagna, A. A.; Cross, V. R.; Kao, J. L. *U.S. Patent* 4 595 668. (c) Van Nordstrand, R. A. *U.S. Patent* 4 547 472.
- (8) Felthouse, T. R.; Murphy, J. A. *J. Catal.* **1986**, 98, 411.
- (9) (a) Huang, T.-N.; Schwartz, J. *J. Am. Chem. Soc.* **1982**, 104, 5245. (b) Huang, T.-N.; Schwartz, J.; Kitajima, N. *J. Mol. Catal.* **1984**, 22, 389.
- (10) Corbin, D. R.; Seidel, W. C.; Abrams, L.; Herron, N.; Stucky, G. D.; Tolman, C. A. *Inorg. Chem.* **1985**, 24, 1800.
- (11) Sohn, J. R.; Lunsford, J. H. *J. Mol. Catal.* **1985**, 32, 325.
- (12) Dessau, R. M. *J. Catal.* **1982**, 77, 304.
- (13) (a) Bergeret, G.; Gallezot, P.; Imelik, B. *J. Phys. Chem.* **1981**, 85, 411. (b) Gallezot, P. *Catal. Rev.—Sci. Eng.* **1979**, 20, 121. (c) Saha, N. C.; Wolf, E. E. *Appl. Catal.* **1984**, 13, 107. (d) Dekewicz, R. P.; Weiss, A. H.; Kranich, W. L. *J. Wash. Acad. Sci.* **1984**, 74, 19. (e) Boudart, M.; Meitzner, G. *Springer Proc. Phys.* **1984**, 2, 217. (f) Dalla Betta, R. A.; Boudart, M. *Catalysis*; North-Holland: Amsterdam, 1973; Vol. 1, p 1329.
- (14) (a) Li, Z.; Mallouk, T. E. *J. Phys. Chem.* **1987**, 91, 643. (b) Persaud, L.; Bard, A. J.; Campion, A.; Fox, M. A.; Mallouk, T. E.; Webber, S. E.; White, J. M. *J. Am. Chem. Soc.*, in press. (c) Li, Z.; Mallouk, T. E.; Persaud, L., submitted for publication.

\* To whom correspondence should be addressed.

by allowing 4,4'-bipyridine to react with excess methyl iodide in acetonitrile, and this compound was converted to the chloride salt hydrate by ion exchange on a Dowex column. This salt was recrystallized from ethanol/water. All other chemicals were reagent grade and were used as received unless otherwise noted.

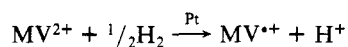
**Platinization of Zeolites L and Y.** Similar procedures were followed for both zeolite types. For platinization using  $\text{Pt}(\text{NH}_3)_4^{2+}$ , the zeolite (7 g) was washed with 800 mL of deionized water (from a Barnstead Nanopure II system, resistivity 18.3 M $\Omega$  cm) and dried at 100 °C in air for 2 days. The zeolite powder was then dispersed by sonication in 1 L of water, and 0.00010–0.24 g of  $\text{Pt}(\text{NH}_3)_4\text{Cl}_2\cdot\text{H}_2\text{O}$  dissolved in 100 mL of water was added dropwise. Stirring of the suspension was continued for 6 h, and the powder was filtered. The sample was repeatedly resuspended in water, centrifuged, and separated from the supernatant until the latter was free of the  $\text{Pt}(\text{NH}_3)_4^{2+}$  UV absorbance at 290 nm. Two methods of reduction of  $\text{Pt}(\text{NH}_3)_4^{2+}$  to  $\text{Pt}^0$  were then used. In the first, the zeolite was carefully dehydrated and reduced with hydrogen, by using conditions specified in ref 8; the hydrogen reduction step was carried out at 300 °C. In the second, the  $\text{Pt}(\text{NH}_3)_4^{2+}$ -exchanged zeolite powder (7 g) was dried under flowing nitrogen at 40 °C for 16 h, suspended in 700 mL of  $\text{H}_2\text{O}$ , and reduced by dropwise addition of 500 mL of 0.1 M aqueous  $\text{NaBH}_4$ . After 8 h, the platinized zeolite was filtered, washed with copious amounts of water, and dried under flowing nitrogen at 40 °C. Samples prepared with higher levels of Pt loading (0.10 mmol/g of zeolite) were light gray; those prepared by smaller amounts of  $\text{Pt}(\text{NH}_3)_4^{2+}$  (0.02 mmol/g of zeolite or less) remained completely white.

Platinization of zeolites Y and L with  $\text{Pt}(\text{acac})_2$  was carried out in a similar fashion; because this complex is insoluble in water, dichloromethane (Fisher, Spectrograde) was used in the loading and subsequent resuspension/centrifugation steps. The zeolite powder (10 g, dried in air at 100 °C for 2 days) was stirred for 4 days with 0.5 g of  $\text{Pt}(\text{acac})_2$  dissolved in 200 mL of dichloromethane. The powder was separated from the supernatant solution by centrifugation and was resuspended in 75 mL of dichloromethane. The last steps were then repeated (10–15 washings were typically required) until the complex was not detectable ( $A_{220\text{ nm}} < 0.02$ ) in the supernatant by UV-visible spectroscopy. The zeolite powder was dried overnight at 40 °C under flowing nitrogen and then heated in air at 225–250 °C for 4 h. After it was cooled to room temperature, the platinized zeolite was reduced with aqueous  $\text{NaBH}_4$  solution and washed as described above for  $\text{Pt}(\text{NH}_3)_4^{2+}$ -exchanged zeolites.

## Results and Discussion

The amount of  $\text{Pt}^0$  deposited inside the zeolite framework, with  $\text{Pt}(\text{acac})_2$  as the source of platinum, is very small. Elemental analyses (Galbraith Laboratories) on hydrated samples establish that the loading level in zeolites Y and L is typically in the range  $(1.0\text{--}3.0) \times 10^{-4}$  mmol of Pt/g; with  $\text{Pt}(\text{NH}_3)_4^{2+}$  as the platinum source, the loading is continuously variable from  $5.0 \times 10^{-5}$  to  $1.0 \times 10^{-1}$  mmol of Pt/g. For the highest loading level, the Pt(111) line is discernible in X-ray powder diffraction patterns, but for samples with less than  $2 \times 10^{-2}$  mmol of Pt/g, the platinum is not detectable by X-ray diffraction, Auger spectroscopy, or X-ray photoelectron spectroscopy. Chemical methods were therefore used to verify the presence of  $\text{Pt}^0$  and to determine its distribution in/on the zeolite particles.

In the presence of  $\text{H}_2$  and  $\text{Pt}^0$ , methylviologen ( $\text{MV}^{2+}$ ) is reduced to the cation radical at pH > 7:



The dicationic  $\text{MV}^{2+}$  exchanges into zeolites L or Y<sup>14,15</sup> to a maximum loading of ca. 1  $\text{MV}^{2+}$  per large cavity (1 per unit cell in L, 8 per unit cell in Y). The excess remains in the solution phase. Because the rate of exchange between zeolite-bound and solution-phase methylviologen molecules is relatively slow, and because the formal potential of the  $\text{MV}^{2+}/\text{MV}^{+\cdot}$  couple is slightly more positive inside the zeolite than in the solution,<sup>14c</sup> zeolites that are platinized only on the inside do not catalyze the rapid reduction of solution-phase  $\text{MV}^{2+}$ . When  $\text{Pt}^0$ /zeolite L prepared from  $\text{Pt}(\text{acac})_2$  was equilibrated with  $\text{MV}^{2+}$ , and hydrogen was then bubbled through the suspension, only the zeolite particles turned blue. The color change typically took 30–60 s in 10 mM  $\text{MV}^{2+}$ /1 mM  $\text{NaHCO}_3$  aqueous solution. The solution phase remained colorless. The blue coloration is characteristic of reduced viologen

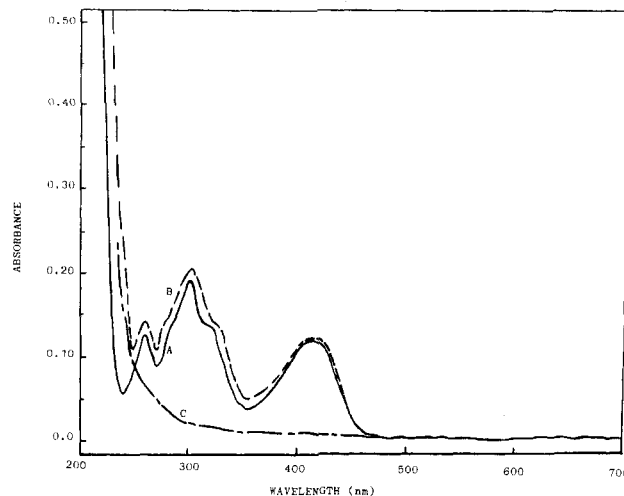


**Figure 1.** UV-visible spectra: (a)  $1 \times 10^{-4}$  M aqueous  $\text{K}_3\text{Fe}(\text{CN})_6$  solution; (B) the same solution after suspension of 10 mg/mL of zeolite L/ $\text{Pt}^0$  prepared from  $\text{Pt}(\text{acac})_2$ , 6-h hydrogen purge, and centrifugation; (C) same as (B), but zeolite L/ $\text{Pt}^0$  prepared from  $\text{Pt}(\text{NH}_3)_4^{2+}$ . The loading of  $\text{Pt}^0$  in (B) and (C) is  $1 \times 10^{-4}$  mmol/g.

radicals,  $\text{MV}^{+\cdot}$ . When zeolite L in which platinum was deposited both internally and externally (prepared from  $\text{Pt}(\text{NH}_3)_4^{2+}$ ) was treated in the same manner, both particles and solution rapidly turned blue. In the latter case, the viologen in the aqueous phase readily contacts the platinum on the outer surface and is reduced. Zeolite Y platinized with either reagent gives blue solutions, even at the lowest level of loading ( $5.0 \times 10^{-5}$  mmol of Pt/g), indicating  $\text{Pt}^0$  both inside and outside. This redox test not only establishes the presence of  $\text{Pt}^0$  but also differentiates between zeolites with platinum inside the cavities and those with platinum both inside the zeolite and on the external surface.

The absence of  $\text{Pt}^0$  on the external surface of zeolite L was verified by an additional chemical test. Ferricyanide,  $\text{Fe}(\text{CN})_6^{3-}$ , a trianionic species, does not enter the anionic framework of zeolites L and Y. This was established from UV-visible difference spectra of ferricyanide solutions equilibrated with the two zeolites. The ferricyanide ion undergoes a rapid reduction to  $\text{Fe}(\text{CN})_6^{4-}$  in the presence of platinum and  $\text{H}_2$  in aqueous solution. Platinum deposited exclusively within the zeolite L framework cannot make contact with ferricyanide when the particles are suspended in a  $1 \times 10^{-4}$  M  $\text{Fe}(\text{CN})_6^{3-}$  solution. UV-visible spectra of these solutions are identical before and after purging for 6 h with hydrogen (Figure 1). For zeolite L containing platinum on both the inner and external surfaces ( $\text{Pt}^0$ /L prepared from  $\text{Pt}(\text{NH}_3)_4^{2+}$ ), the identical treatment results in complete disappearance of the absorbance maxima at 302 and 418 nm attributable to the ferricyanide ion (Figure 1). Again, zeolite Y platinized by either method and reduced with either hydrogen or aqueous  $\text{NaBH}_4$  shows evidence for  $\text{Pt}^0$  on the outer surfaces, as it catalyzes the  $\text{Fe}(\text{CN})_6^{3-}$  reduction. The ferricyanide test is preferred for zeolite Y, since diffusion of  $\text{MV}^{+\cdot}$  out of zeolite Y is known to be fast,<sup>15</sup> and false positive tests for external Pt might be obtained by using the  $\text{MV}^{2+}$  test.

In order to determine the sensitivity of the ferricyanide test, we prepared nonporous  $\text{SiO}_2$  powder (made by grinding quartz glass to an average particle size of 5  $\mu\text{m}$ ) impregnated with  $\text{Pt}(\text{acac})_2$ , dried, and reduced as above for zeolites Y and L. With  $\text{SiO}_2$  as the support,  $\text{Fe}(\text{CN})_6^{3-}$  reduction was observable in 12 h with platinum loadings of  $(3\text{--}5) \times 10^{-7}$  mmol of Pt/g but not with loadings 1 order of magnitude lower. This result suggests (assuming similar degrees of Pt dispersion on the external surfaces of zeolite L and  $\text{SiO}_2$ ) that zeolite L platinized with  $\text{Pt}(\text{acac})_2$  has less than 0.1% of its platinum on the external surface.

We have described a new method for depositing platinum exclusively on the inner surfaces of zeolite L particles. The same selectivity is not observed for zeolite Y, even though the crystallographic channel diameters in Y and L (7.4 and 7.1 Å, respectively) are quite similar.<sup>16</sup> The difference between zeolites

(15) Gemborys, H. A.; Shaw, B. R. *J. Electroanal. Chem. Interfacial Electrochem.* 1986, 208, 95.

Y and L, with regard to platinization on the external surface, can probably be attributed to the connectivity of the large cages in the two structures. In the zeolite Y structure, each supercage has four nearest neighbors and molecular diffusion can occur freely in three dimensions. In zeolite L, however, the large cavities are linearly interconnected to from one-dimensional tunnels; diffusion of large molecules such as Pt(acac)<sub>2</sub> is likely to be severely restricted. Hence it is possible with the L structure to wash the complex completely off the external surface and to dry the zeolite before substantial diffusion out of the bulk and onto the external surface can occur. The chemical tests outlined above are inexpensive and sensitive and may be of general utility in locating noble-metal catalysts in/on zeolites.

**Acknowledgment.** We thank Dr. Michael Schmerling, Department of Mechanical Engineering, The University of Texas at Austin, for carrying out the SEM measurements. This work was supported by a grant from the Gas Research Institute.

**Registry No.** Pt, 7440-06-4; Pt(acac)<sub>2</sub>, 15170-57-7; MV<sup>2+</sup>·2Cl<sup>-</sup>, 1910-42-5; Fe(CN)<sub>6</sub><sup>3-</sup>, 13408-62-3.

(16) Meier, W. M.; Olson, D. H. *Atlas of Zeolite Structure Types*; Juris Druck + Verlag AG: Zurich, 1978; pp 37, 59.

Contribution from the Departments of Chemistry, Texas A&M University, College Station, Texas 77843, and University of Delaware, Newark, Delaware 19716

### Insertion Reactions of Carbon Dioxide with Square-Planar Rhodium Alkyl and Aryl Complexes

Donald J. Darensbourg,<sup>\*1a</sup> Georg Grötsch,<sup>1a</sup> Philip Wiegrefe,<sup>1a</sup> and Arnold L. Rheingold<sup>1b</sup>

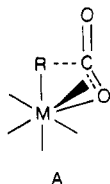
Received April 24, 1987

Mechanistic aspects of carbon-carbon bond forming reactions resulting from the insertion of carbon dioxide into metal-carbon bonds have been the focus of our recent attention (eq 1).<sup>2</sup> The



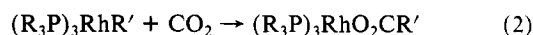
importance of reaction 1 stems from the fact that it constitutes a fundamental step in the use of carbon dioxide as a feedstock for organic chemicals.<sup>3</sup>

Comparative studies between carbonylation and carboxylation reactions based on investigations involving group 6 metal carbonyl alkyl and aryl derivatives of the type RM(CO)<sub>5</sub> (M = Cr, W) have been completed.<sup>4</sup> It was found that the two processes differ markedly with respect to several reaction variables. For carboxylation reactions a concerted process involving a transition state as shown in A was proposed on the basis of the following ob-



servations: (i) the reaction is first order in both CO<sub>2</sub> and metal substrate, (ii) activation parameters are indicative of an I<sub>a</sub> mechanism involving a great deal of bond making in the transition state, (iii) CO<sub>2</sub> insertion into the W-C bond was not retarded by excess CO (that is, the process does not involve a coordinatively unsaturated intermediate), (iv) upon increasing the nucleophilicity of the metal center, the rate of carboxylation is enhanced, and (v) the configuration at the alkyl carbon center is retained.<sup>5</sup>

This report contains further observations on the insertion reactions of CO<sub>2</sub> into the Rh-C bond of several Rh(I) complexes in an attempt to better define the reaction parameters for these processes. Specifically, studies have centered on square-planar complexes of rhodium of the general formula (R<sub>3</sub>P)<sub>3</sub>RhR', where R and R' = alkyl or aryl groups. Two primary reasons for investigating reaction 2 mechanistically are (a) these species rep-



resent the best cases for possibly observing CO<sub>2</sub> coordination to the metal center prior to carbon-carbon bond formation and (b) square-planar complexes are of increasing importance in stoichiometric and catalytic synthesis of organic chemicals.<sup>6</sup>

### Experimental Section

All manipulations were carried out either in an argon drybox or on a double-manifold Schlenk vacuum line, using freshly distilled solvents. Reagent grade benzene, toluene, and hexane were purified by distillation under nitrogen from sodium benzophenone ketyl. Me<sub>3</sub>P was purchased from Strem Chemicals, Inc. (Newburgport, MA 01950). (Ph<sub>3</sub>P)<sub>3</sub>Rh-Ph,<sup>7</sup> (Ph<sub>3</sub>P)<sub>3</sub>Rh-Me,<sup>7</sup> (Me<sub>3</sub>P)<sub>3</sub>Rh-Me,<sup>8</sup> (Ph<sub>3</sub>P)<sub>2</sub>(CO)Rh-Me,<sup>9</sup> and (Ph<sub>3</sub>P)<sub>2</sub>(CO)Ir-Me<sup>10</sup> were prepared by the methods previously described. Proton NMR spectra were recorded on a Varian EM-390 spectrometer, whereas <sup>13</sup>C and <sup>31</sup>P NMR spectra were obtained on a Varian XL-200 spectrometer. Infrared spectra were determined on Perkin-Elmer 283B and IBM FTIR/85 or FTIR/32 spectrometers. GC experiments were performed with a Perkin-Elmer Sigma 2 gas chromatograph. The high-pressure infrared measurements were carried out on the IBM FTIR/85 spectrometer using a high-pressure IR cell (CIR cell, ZnSe) provided by Barnes Analytical. The reaction was carried out in a 300-mL Parr reactor connected to the CIR cell by 1/16-in. stainless steel tubing. The sample was delivered directly from the reactor to the cell with both maintained at the pressure of the reactor. Background spectra were determined in a completely analogous manner.

Elemental analyses were obtained by Galbraith Laboratories, Knoxville, TN.

**(Benzoato)tris(triphenylphosphine)rhodium(I) (2).** A 0.2910-g (0.3010-mmol) amount of (Ph<sub>3</sub>P)<sub>3</sub>Rh-Ph (1) in 3 mL of benzene was reacted with CO<sub>2</sub> at a pressure of 300 psi for 24 h. Evaporation of the solvent afforded orange-red, microcrystalline 2: yield 0.3159 g (98%); IR (C<sub>6</sub>H<sub>6</sub>) ν(OC)<sub>as</sub> 1608 (m), 1571 (m), ν(CO) 1354 (s), ν(C-C<sub>ar</sub>) 1585 (w), 1500 (w), 1465 (w), 1435 (vs) cm<sup>-1</sup>.

**Tris(trimethylphosphine)phenylrhodium(I) (4).** To a suspension of 0.3100 g (0.7003 mmol) of [(Me<sub>3</sub>P)<sub>3</sub>Rh]Cl (3) in 35 mL of toluene was added at -60 °C 0.0706 g (0.8404 mmol) of PhLi dissolved in ether/hexane. Upon slow warming to 0 °C, formation of 4 was indicated by the solvation of 3. After 1 h of stirring at 0 °C to complete the production of 3, the reaction mixture was filtered through Celite. After removal of the solvent at 0 °C, the resulting orange solid was redissolved in 10 mL of hexane, the solution filtered again through Celite, and the solvent evaporated until crystallization started. Following a brief warming to 40 °C, the clear solution was slowly cooled to -11 °C. After 4 days at -11 °C, orange crystals were obtained and isolated by filtration: yield 0.2100 g (74%); <sup>1</sup>H NMR (C<sub>6</sub>D<sub>6</sub>) δ 7.93 (m, 2 H, C<sub>6</sub>H<sub>5</sub>), 7.22 (m, 3 H, C<sub>6</sub>H<sub>5</sub>), 1.17 (m, 9 H, H<sub>3</sub>CP), 1.03 (m, 18 H, H<sub>3</sub>CP); <sup>13</sup>C{<sup>1</sup>H} NMR

- (1) (a) Texas A&M University. (b) University of Delaware.
- (2) (a) Darensbourg, D. J.; Rokicki, A. *J. Am. Chem. Soc.* **1982**, *104*, 349. (b) Darensbourg, D. J.; Kudarski, R. *J. Am. Chem. Soc.* **1984**, *106*, 3672.
- (3) (a) Eisenberg, R.; Hendriksen, D. E. *Adv. Catal.* **1979**, *28*, 79. (b) Sneed, R. P. A. In *Comprehensive Organometallic Chemistry*; Wilkinson, G., Stone, F. G. A., Abel, E. W., Eds.; Pergamon: Oxford, U.K., 1982; Vol. 8, p 225. (c) Ito, T.; Yamamoto, A. *Organic and Bio-Organic Chemistry of Carbon Dioxide*; Inoue, S., Yamazaki, N., Eds.; Kodansha: Tokyo, Japan, 1982; p 79. (d) Darensbourg, D. J.; Kudarski, R. *Adv. Organomet. Chem.* **1983**, *22*, 129.
- (4) Darensbourg, D. J.; Hanckel, R. K.; Bauch, C. G.; Pala, M.; Simmons, D.; White, J. N. *J. Am. Chem. Soc.* **1985**, *107*, 7463.

- (5) Darensbourg, D. J.; Grötsch, G. *J. Am. Chem. Soc.* **1985**, *107*, 7473.
- (6) (a) See Chapter 3 in ref 3c and references contained therein. (b) Carmona, E.; Palma, P.; Paneque, M.; Poveda, M. L. *J. Am. Chem. Soc.* **1986**, *108*, 6424. (c) Fujiwara, Y.; Kawata, I.; Sugimoto, H.; Taniguchi, H. *J. Organomet. Chem.* **1983**, *256*, C35. (d) Fujiwara, Y.; Kawachi, T.; Taniguchi, H. *J. Chem. Soc., Chem. Commun.* **1980**, 220. (e) Sugimoto, H.; Kawata, I.; Taniguchi, H.; Fujiwara, Y. *J. Organomet. Chem.* **1984**, *266*, C44.
- (7) Keim, W. *J. Organomet. Chem.* **1968**, *14*, 179.
- (8) Jones, R. A.; Mayor Real, F.; Wilkinson, G.; Galas, A. M. R.; Hursthouse, M. B. *J. Chem. Soc., Dalton Trans.* **1981**, 126.
- (9) Dahlenburg, L.; Mirzaei, F.; Yardimcioglu, A. Z. *Naturforsch., B: Anorg. Chem., Org. Chem.* **1982**, *37B*, 310.
- (10) Dahlenburg, L.; Nast, R. *J. Organomet. Chem.* **1974**, *71*, C49.